Silicon nanoparticles: a new and enhanced operational material for nitrophenol sensing

Rizwan Wahab, Naushad Ahmad & Manawwer Alam

Journal of Materials Science: Materials in Electronics

ISSN 0957-4522

J Mater Sci: Mater Electron
DOI 10.1007/s10854-020-04269-8

Springer

J Mater Sci: Mater Electron

Silicon nanoparticles: a new and enhanced operational material for nitrophenol sensing

Rizwan Wahab[1,*], Naushad Ahmad[2], and Manawwer Alam[2]

[1] Department of Zoology, College of Science, King Saud University, P.O. Box 2455, Riyadh 11451, Saudi Arabia
[2] Department of Chemistry, College of Science, King Saud University, P.O. Box 2455, Riyadh 11451, Saudi Arabia

Received: 7 May 2020
Accepted: 17 August 2020

ABSTRACT

The environmental problem is a big issue in the current scenario because the human beings are affected via natural or manmade sources. Over a range of industrial pollutents, the nitrophenol (referred to as 4-NP) known as harmful industrial chemical for the environment and listed as a carcinogenic compound for human health. To keep this view the present manuscript describes the formation of highly crystalline silicon nanoparticles (Si-NPs) and applied for the electrochemical sensing of 4-NP. The Si-NPs exhibit numerous applications in various directions such as catalyst, solar cells, LEDs, batteries etc. The Si-NPs were formed from the physical approach with using argon-silane mixture in a gas chamber with impregnation of microwave plasma. The processed material was examined through various techniques such as X-ray diffraction pattern (XRD), field emission scanning electron microscopy (FESEM), transmission electron microscopy (TEM) and Fourier transform spectroscopy (FTIR). It reveals from the acquired analysis that the size of each NP is ~ 4 nm with good structural and chemical characteristics and applied as a film form against to check the sensing of 4-NP with three electrode system. The electrochemical studies were conducted through cyclic voltammetry (CV) in terms of their low to high concentration (7.8, 15.62, 31. 25, 62.25, 250, 500, 1000 μM in PBS), scan rate at variable potential was accessed from 5 to 100 mV with Si-NPs based electrode. The sustainability, reproducibility and efficacy of the formed sensor (Si-NPs/GCE) was examined in occurrence with 4-NP (62.25 μM) for seven consecutive cycles. Including to this, chronoamperometry (0 to 1500 *s*) and electrochemical impedance spectra (7.8–1000 μM in PBS) were also analyzed. On the basis of acquired results and discussion a probable mechanism was also described.

Address correspondence to E-mail: rwahab05@gmail.com; rwahab@ksu.edu.sa

https://doi.org/10.1007/s10854-020-04269-8
Published online: 31 August 2020

1 Introduction

In the recent past, there is an enhanced discharge of pollutants through man-made such as organic, inorganic, industrial, households and various other means etc., also natural are a severe threat to the ecosystem generated in water and atmosphere [1]. A specific, fast and furious methods are required to measure the pollutants, which are responsible for the obliteration for the ecosystem. Among various organic pollutants, the phenolic derivatives (such as nitrophenols, bisphenol, nanylphenol 9 etc.) are found to be a hazardous material to the ecosystem even at a very low concentration of traces levels [2]. Out of others phenolic derivatives, the 4-nitrophenol ($C_6H_5NO_3$, 4-NP), which is widely utilized as a plasticizers, pesticides, pharmaceutical, explosives, dyes etc.; are extremely prevalent in environment [3]. Including the plastic industry, the 4-NP is also utilized in tannery, fungicide, pH indicator in chemical laboratories etc. [4]. The toxicity of compound is very high and, on the basis of their severe toxicity rate, USEPA (United state environmental protection agency) classified the 4-NP as a major pollutant with maximum permissibility of 60 ppb (0.43 μM) in drinking water [5]. To overcome these obstacles, there is an urgent need for the detection and quantification of 4-NP through cost effective, fast, precise and reliable analytical tools [5]. For the environmental safety aspects, the detection of phenols and phenolic derivatives in normal water and their effluents are major concern because it expresses a toxic effect on animals, humans, plants etc. The oxides based semiconductor materials, polymers, nanocomposites are the selective materials for the development of efficient chemical sensor, which is an important issue for the detection, and quantification of organic pollutants, toxic chemicals and materials [6, 7]. Although the available techniques provides the advantages of sensitivity and accuracy but their way of sample preparation, difficulties in analysis, longer analysis time, necessity of molecules derivatization, higher cost etc. are the factors, which limits their utility [8]. For the degradation of organic molecules (p-nitrophenol), some methods have been adopted such as biodegradation [9], photocatalytic [10], microwave assisted oxidation [11], electrocatalytic oxidation [12] and photoelectrocatalytic degradation [13, 14] etc. Over various methods of nitrophenol detection, electrochemical techniques supported via the direct determination of phenols with signals, which are recovered from the reduction of nitrogroup in 4-NP. Towards this direction, enormous applications related to the electroanalytical based microelectrode were employed as a working electrode for the detection and quantification of amine absorbed with phenol through metal (nanoporous gold), metal oxides [zirconia (ZrO_2) nanoparticles] and carbon based materials (multiwalled carbon nanotubes) [15–17] etc.

The 4-NP can be reduced exclusively with the use of catalytic evaluation of metal NPs in aqueous suspensions. While most evaluations deal with colloidal metal (Cu, Ag, Au, Pt, Pd, Ru) nanoparticles [18–24]. A range of techniques have been employed for the detection of 4-NP such as spectrophotometry [25], fluorescence [26] liquid and gas chromato graphy (HPLC & GC) [27, 28], electrophoresis [29] etc. But these techniques needs extensive care and require expensive chemical reagents with good expertise to handle them. It is required and urgent demand for the development of modern technique, which have simple operational method, low preparation cost, less time consuming, fast and efficient detection of 4-NP. The electrochemical techniques is a best technique to solve these problems and can be easily overcomes these shortcomings, also to permit a sensitive, selective and reproducible determination of analyte [30].

Over a long range of metal oxides nanostructures, the silicon nanoparticles (Si-NPs), exhibit larger applications in various directions such as light emitting diodes, dye sensitized solar cells, lithium ion batteries, anti-static films, coatings, imaging, energy storage and catalyst etc [31]. The Si nanostructures can be synthesized through various ways such as chemical solution, ball milling, hydrothermal, reverse micelle process and various others [32]. The solution/chemically grown materials have advantage to produce nanostructures in a bulk amount with a cost effective manner but the high quality and crystallinity are a matter of concern for silicon nanostructures. The material can also be prepared from the physical ways such as thermal decomposition (TE), laser ablation, vapor-phase thermal decomposition, vapor-phase thermal decomposition, inert gas condensation, pulse vapor deposition (PVD), laser and flush spray pyrolysis, electro sprying [33, 34] etc. The present work demonstrates the formation of Si-NPs with the use of microwave plasma reactor; to this reactor the argon-silane mixture was introduced to

the reaction chamber with hydrogen gas. The argon-silane mixture was decomposes through the microwave irradiation and it gives high crystalline Si-NPs. The processed material was well characterized in terms of their crystalline, morphological and chemical characteristics. Out of these analyses of NPs, the materials sensing characteristics were observed against nitrophenol (4-NP) with various parameters such as effect of concentration, effect of potential, scan rates, chronoampherometric response and electrochemical impedance spectroscopy (EIS) were measured with modified Si-NPs/GCE electrode. Also, based on the acquired results and their discussions experimental details with mechanism were also presented.

2 Materials and methods

2.1 Experimental

2.1.1 *Formation of silicon nanoparticles (Si-NPs) through microwave plasma reactor*

For the formation of Si-NPs microwave plasma reactor was utilized. At the reaction compartment, a specific amount of argon-silane mixture 1% SiH_4 (purchased from Aldrich chemical corporation, U.S.A) and 99% O_2 was presented [34–36].The silane (SiH_4) was decomposes from the microwave energy, which has high frequency ~ 2.5 GHz and 2000 W power and was joined with gas flow to originate the plasma. In this plasma generator the pressure was maintained to ~ 30 mbar in the plasma chamber. Once the plasma enters into the chamber silane was dissociated into silicon and hydrogen (Institute for Combustion and Gasdynamics, University of Duisburg-Essen, Duisburg). The plasma flows at lower temperatures, where the particle grows through Brownian coagulation, amalgamation and give a surface growth [34–36]. The plasma treated powder was examined for the basic characterization.

2.1.2 *Materials characterization*

The recovered powder was categorized in detail; such as FESEM (Hitachi, Tokyo, Japan) and TEM (JEM JSM 2010 from JEOL at 200 kV, Tokyo, Japan) for structural detail correspondingly. For FESEM analysis, the processed powder was sprayed on the carbon tape and mounted on the sample holder. The coated sample was transferred to the sputtering chamber for good quality image and to avoid the charging effect during examination of FESEM sample. The sputtering was conducted with osmium tetraoxide (OsO_4) for ~ 3 s on the surface of nanopowder. Once the sputtering was accomplished, the sample holder was fixed to the FESEM instrument and analyzed. In addition to this, the morphological analysis was further accessed from TEM equipped with HR-TEM facility. Very small amount of powder (~ 1–2 mg) was dissolved in ethanol (~ 50 mL) and sonicated in a glass beaker in bath sonicator (cole parmer, USA) for ~ 10 min. Once the sample was completely sonicated, to this suspension solution a carbon coated copper grid (Aldrich chemical corporation, U.S.A) was dipped for 3 *s*, removed it from the solution and dried it at room temperature. Thereafter, it was fixed in sample holder of TEM and analyzed at 200 kV. The X-ray powder diffractometer (XRD, Rigaku, Japan) with $Cu_{K\alpha}$ radiation ($\lambda = 1.54178$ Å, angle 20° to 80° with 6°/min) was analyzed. The powder particles functional characteristics were examined through Fourier transforms infrared (FTIR, Perkin Elmer, USA, ranges from 4000 to 400 cm^{-1}).

2.2 Si-NPs based sensor based with glassy carbon electrode (Si-NPs/GCE)

The grown powder of Si-NPs was used as a film form and pasted on glassy carbon electrode (GCE), to sense the 4-NP in phosphate buffer solution (PBS, 0.1 M pH 7.2). For an electrode preparation, a layer of the prepared powder (Si-NPs) was coated on GCE electrode with the utilized area ($71\,10^{-3}$ cm^2). A pinch of Si-NPs were mixed with butyl carbitol acetate (BCA) with a specified ratio (70 & 30%) and then the processed slurry was coated as a film of Si-NPs on GCE electrode, the GCE was dried at 60±5 °C for 30 min to get a uniform layer over entire surface of electrode. The electrochemical analysis was conducted with the prepared electrode through autolab potentiostat/galvanostat, PGSTAT 204-FRA32 control with NOVA software (Metrohom Autolab B.V. Kanaalweg 29-G, 3526 km Utrecht, Nether lands) with three electrode system [37, 38]. The Si-NPs/GCE electrode was used as a working electrode, whereas a platinum (pt) wire was castoff as a counter and Ag/AgCl (sat.KCl) was used as a reference electrode

consequently. The PBS (0.1 M; pH 7.2) with 4-NP was used as an analyte solution for the whole electrochemical study. For to check, the sensing property of 4-NP with Si-NPs/GCE a wide range of different concentration of 4-NP (7.8, 15.62, 31.25, 62. 25, 250, 500 and 1000 μM/100 mL in PBS) was adopted and test from −1.5 to+1.5 V current. The effect of scan rates (4-NP (62.25 μM) at different potentials (5 to 100 mV) were accessed. The reproducibility and reliability test were also conducted for a longer period (One to 30 days). Including this, the amperometry test was also performed from 0 to 1500 *s* for 4-NP in PBS, the electrochemical impedance at different concentrations of 4-NP (7.8, 15.62, 31.25, 62.25, 250, 500 and 1000 μM) with current–time (i−t) curves were measured at a set potential in PBS solution.

3 Result and discussion

3.1 X-ray diffraction pattern (XRD)

The XRD was accessed as described the procedure in Sect. 2.1.2 for to know the product crystallinity, size and phases respectively. As received spectrum from XRD (Fig. 1), shows very well defined peaks are seen related the available data of powder sample and matched with the JCPDS card No. 39-1346. The peaks positions are as 28.40 <111>, 47.20 <220>, 56.05 <311>, 69.10 <400> and 76.30 <331> are clearly indexed with silicon phase (Si-NPs). The each crystallite dimension was estimated through the well-known scherror equation, which reveals that the size is very small (∼4 nm). There is no other peaks related to any impurities had been observed in the spectrum, which states that the processed material is highly pure and well crystalline in nature [39, 40].

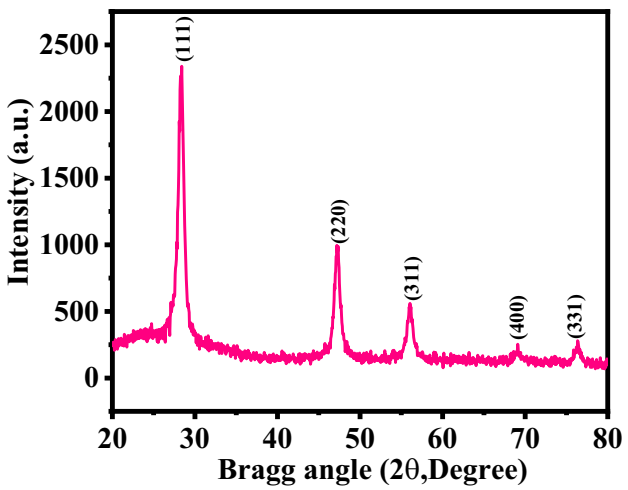

Fig. 1 The XRD pattern of processed silicon nanoparticles (Si-NPs)

3.2 Structural detail of Si-NPs (FESEM and TEM results)

The formed powder was analyzed through the FESEM as described in Sect. 2.2 for to know the structural detail of nanopowder. The captured images (Fig. 2), illustrates the structural detail of formed nanostructures. From the images (Fig. 2a and b), it reveals that several tiny small spherical shaped nanoparticles (NPs) are seen in a specified area, which are either single or in a grouped and jointed with other NPs. The surfaces and morphologies are very clear, smooth and spherical in shape. The average diameter of each NP is ∼4 nm in size. The average size of particle was estimated through the size distribution measured with the use of the ImageJ software package, which showed that the size of each QD is ∼3.88 nm with 23% of polydispersity (Fig. 2b, inset). Further for more clarification, the observation related to the morphology of the grown nanostructure, TEM was utilized and the received data is presented as Fig. 2c and d. As from the FESEM, very similar observation was also received from TEM and it reveals that many tiny particles are arranged in the center, spherical in shape, and some are jointed with other. The average diameter of each particle is ∼4 nm is visualized. The high resolution image was also examined (Fig. 2d), which consist the high crystalline property of the material and fringes distance apart from ∼0.233 nm between the lattices (Fig. 2d), which is corresponding to the previously published literature [41, 42]. The TEM analysis (Fig. 2c and d) is consistent with the FESEM images (Fig. 2a and b) [41, 42].

3.3 The FTIR results of Si-NPs

The functional characteristics of Si-NPs were examine through FTIR spectroscopy ranges from 400 to 4000 cm^{-1}. For to analyze this, a certain amount of rich brown colored powder was mixed well with the potassium bromide (KBr) and the mixture was compressed with high-pressure [∼4 tons (*t*)] to form a pellet. The pellet was fixed to a sample holder and

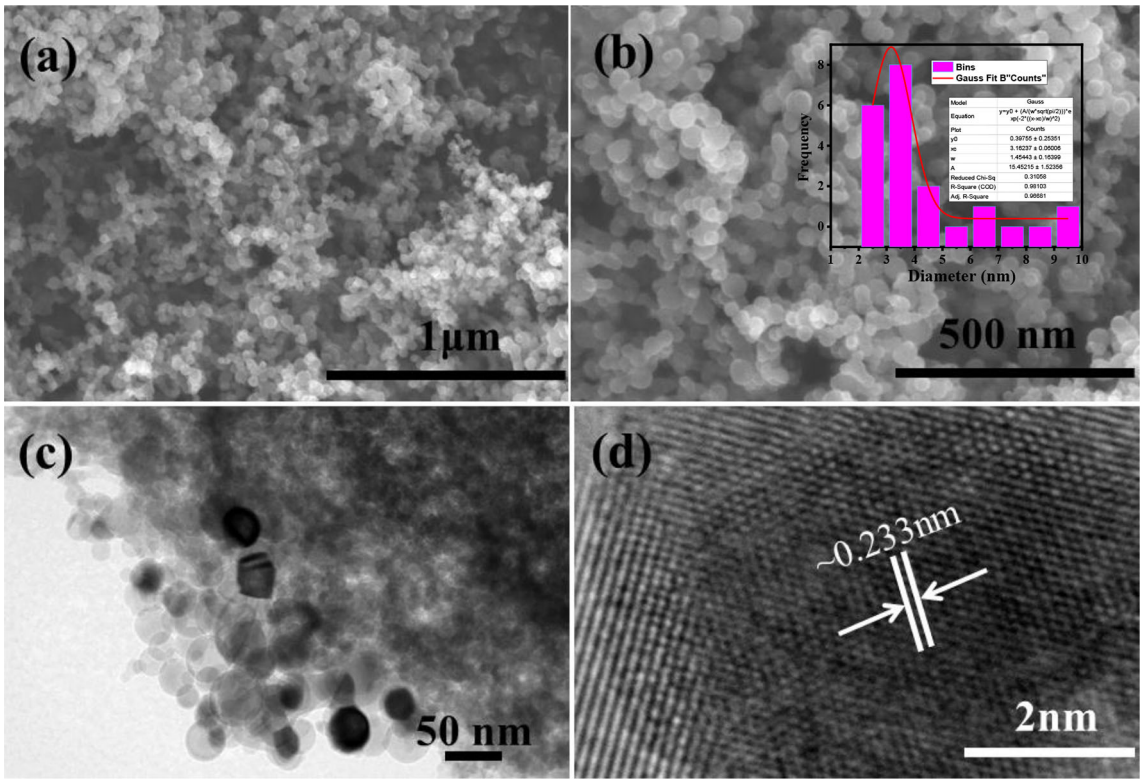

Fig. 2 The powdery spherical nanostructure shows at low (**a**) and high (**b**) magnification FESEM images of Si-NPs respectively. Size distribution of prepared Si-Nanoparticles (~ 3.88 nm **b**), poly disparity ~ 23%) with ImageJ software. **c** and **d** Shows the TEM & HR-TEM of Si-NPs respectively, which gives the general morphology of the prepared NPs and their fringes distance between two lattices (~ 0.233 nm)

measured the FTIR spectroscopy. The FTIR spectroscopy of Si-NPs (Fig. 3) shows the atmospheric oxygen trapped to the particles surfaces and it can be clearly seen through the vibrational modes of oxides. A wide band at 1199 cm^{-1} ascends, which is due to Si–O-Si stretching mode of ambiances on metal oxide (Si) surfaces. The small sharp bands were also observed at 2246 cm^{-1} and at 881 cm^{-1}, denoting the H-SiO_3 stretching and bending vibration mode, respectively. The silicon hydride (Si-Hx (x=1–3) or hydrogen terminated silicon band on the surface of silicon was observed at 2090 cm^{-1} [39–42].

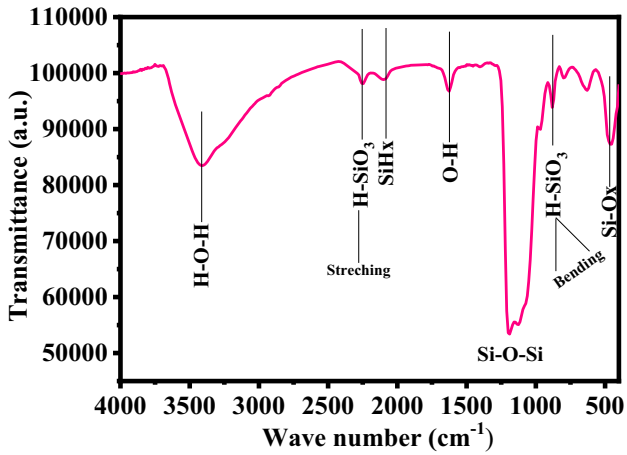

Fig. 3 The FTIR spectra of microwave assisted plasma processed Si-NPs

3.4 Cyclic voltammetry (CV) studies of Si-NPs with and without coated electrode.

The electrochemical studies was accomplished with cyclic voltammetry (CV) and checked whether the charge is present on coated (with NPs) and uncoated/bare electrode on GCE. To examine this initially, the uncoated electrode was (without Si-NPs on GCE) tested in presence of 4-NP [500 M/100 mL PBS (0.1 M, pH 7.2)] solution with the scan rate of 100 mV/s. The acquired spectrum denotes that there is no any peak was observed, which indicates that the bare electrode doesn't have any redox potential on the surface. Once the Si-NPs layer was coated on GCE

and to make the modified electrode (Si-NPs/GCE) and tested for electrochemical examination in presence of 4-NP at concentration [500 μM/100 mL PBS (0.1 M, pH 7.2)], it shows a change in anodic and cathodic peak. The received data shows that the working/modified electrode (Si-NPs/GCE) support the electron transportation and sense the 4-NP (500 μM), which act as a analyte in presence of PBS [43]. The spectra denotes the oxidation and reduction potential were observed at $1.44\,10^{-4}$, and $-1.22\,10^{-4}$ V in presence of 4-NP respectively [44], and confirms that highly crystalline film of Si-NPs coated on GCE (Si-NPs/GCE) is much efficient to oxidizes the 4-NP and also responsible for the electron transportation in PBS solution (Fig. 4) [44].

3.5 Effect of 4-NP concentration on modified electrode (Si-NPs/GCE)

To know the effect of current and potential (I–V) on processed working electrode (Si-NPs/GCE), a range of different concentrations of 4-NP (7.8, 15.62, 31.25, 62.25, 250, 500 &1000 μM/100 mL PBS) were chosen and checked the CV in PBS and the obtained data is presented as Fig. 5. From the obtained graph its shows that a chronological change was observed in the oxidation and reduction peaks from a low to high range of 4-NP concentration solution. In this the potential window was opted in range from −1.5 to+ 1.5 V. The spectral data illustrated as Fig. 5, which states that the current is increases with the enhancement of 4-NP concentration and this is directly related with anodic peak and consistent with 4-NP concentration. It may imagine that once the current was increases with increase of 4-NP concentration, and directly proportional to the rate of electrons transportation at the conduction band (Fig. 5) [45, 46].

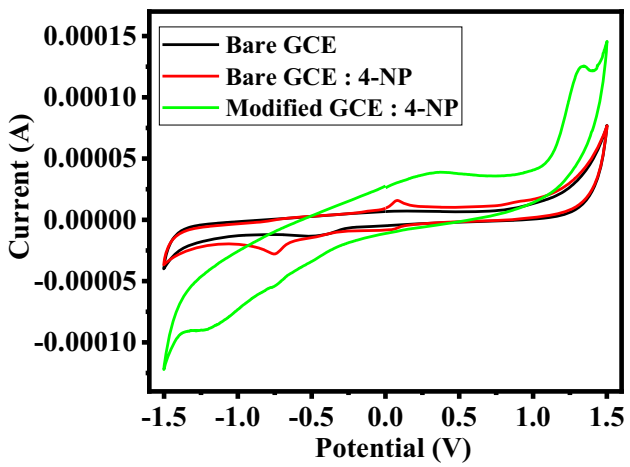

Fig. 4 Cyclic voltammograms of bare and modified electrodes in absence and presence of 4-NP (500 μM) in 0.1 M phosphate buffer (pH 7.2). Scan rate: 100 mV/s

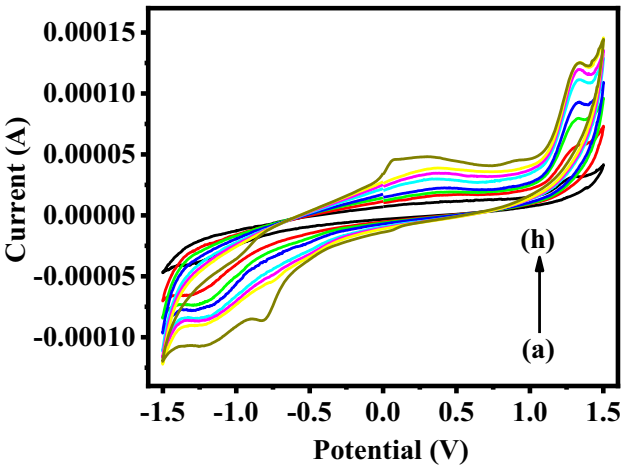

Fig. 5 Cyclic voltammetric responses of Si-NPs in 0.1 M phosphate buffer at different concentrations of 4-NP (a–h 7.8, 15.62, 31.25, 62.25, 250, 500 and 1000 μM)

3.6 Effect of potential at Si-NPs/GCE electrode

The enactment of Si-NPs/GCE in response to reproducibility and reliability, the different potential ranges (5, 10, 20, 30, 40, 50, 60, 70, 80, 90 and 100 mV/s) were chosen and sensing was accomplished in PBS solution (Fig. 6). A sequential change/responses were observed at different cycles at a fixed concentration of 4-NP in PBS at pH 7.2. The acquired data reveals that the effect of potential on the formed electrode, at initial very low potential (5 mV/s), displayed not much response was observed in the oxidation and reduction peaks it might be the possibility of electron displacement is very less at a specified potential. The observation indicates that at a very low potential, less current signals in terms of oxidation and reduction were observed whereas once the potential was increased gradually in the solution, the cyclic responses (redox) were increases, this attributes that the processed Si-NPs/GCE electrode is functional for the larger scale potential range and Si-NPs easily sense the 4-NP in PBS solution [45, 46]. Based on the obtained CV graph with different potential range a linear plot was constructed for the examination of ionization potential at cathode (IPc) and anode (IPa)

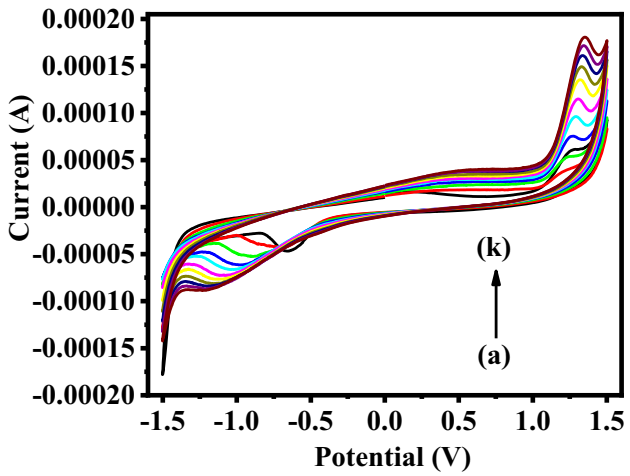

Fig. 6 Cyclic voltammetric responses of Si-NPs in the presence of 4-NP (62.25 μM) as a function of scan rates (a–k 5, 10, 20, 30, 40, 50, 60, 70, 80, 90 and 100 mV)

with the assessment of correlation coefficient (R^2). From the graph it reveals that in both (IPc & IPa) for Si-NPs/GCE, the value of R^2 were 0.999 and 0.993 respectively (Fig. 7). Apart from this, the detection limit (LOD) for Si-NPs/GCE (IPc) and (IPa) were assessed which were 0.512 and 0.614 respectively. The limit of quantitation (LOQ) for Si-NPs/GCE (IPc) and (IPa) evaluated which were 1.55 and 1.86 respectively (Table 1).

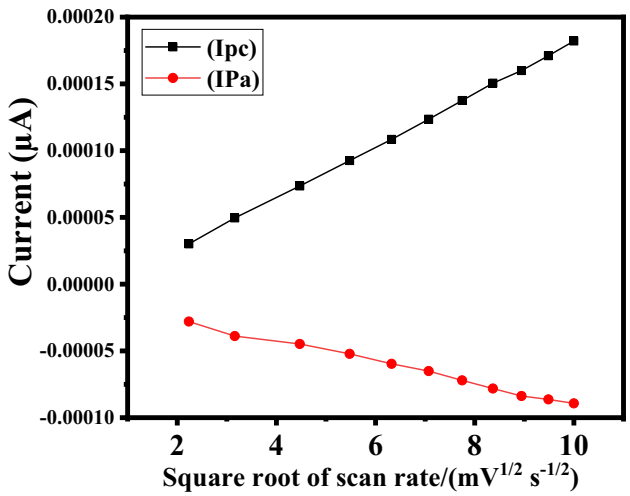

Fig. 7 Liner calibration graph for cathode and anode potentials of Si-NPs/GCE

3.7 Consecutive cycle's response for Si-NPs/GCE electrode

The modified Si-NPs/GCE electrodes sensors stability, reliability and reproducibility were examined in terms of their cycle responses and the received data is presented as Fig. 8a and b. The spectra shows the seven successive cycles of Si-NPs/GCE electrode in presence of 4-NP (62.25 M, in 0.1 M PBS) analyzed at 100 mV/s. The cycles graphs illustrates the excellent reproducibility in presence of 4-NP and the data were learned from first day to till 7 days and to retain the chemical and physical properties of the processed sensor (Fig. 8a). The formed sensor was stored in an ambient atmosphere, the changes in the voltammetric cycles were further confirms for longer stability and reproducibility. The stability of the formed sensor was further tested for 1 month and it doesn't receive any much change in the cycle's responses, this again authorizes that the processed electrode possessed satisfactory and greater reproducibility (Fig. 8b). The acquired data sanction that the Si-NPs/GCE electrode has enhanced stability along with good reproducibility, sustainable for longer periods and applicable for practical uses [46, 47]. The relative standard deviation (RSD) and stability were calculated to be 1.154% 14.9%, which again justifies that the formed exhibit a substantial reproducibility.

3.8 Chronoamperometry of the processed Si-NPs/GCE electrode with 4-NP

The chronoamperometry is a time reliant technique, where the potential is applied to the working electrode in stages rather than continuously. The current received from the faradaic processes arose at working electrode and scrutinized as a function of time. The analytes fluctuates towards the solution on the outward of processed sensor. In this case, the current–time reliant study was performed for the dispersal and well-ordered process occurred at modified electrode (Si-NPs/GCE) and changes with the custom of analyte concentration (4-NP). The present spectra show a specified time intervals under a set voltage (Fig. 9). Here the time responses vs potential was measured from 0 to 1500 *s* to check the working electrode (Si-NPs/GCE) sensors selectivity & reproducibility. Serial responses were observed with respect to time for Si-NPs/GCE with respect to 4-NP. At 0 *s* current response was very less ($-6.985\,10^{-4}$) but

Table 1 Limit of detection (LOD) and Limit of quantification for Si-NPs/GCE

S. no.	Nanostructure	LOD (μM)	LOQ (μM)	Correlation coefficient (R^2)
1	Si-NPs/GCE (IPa)	0.614	1.86	0.993
2	Si-NPs/GCE (IPc)	0.512	1.55	0.999

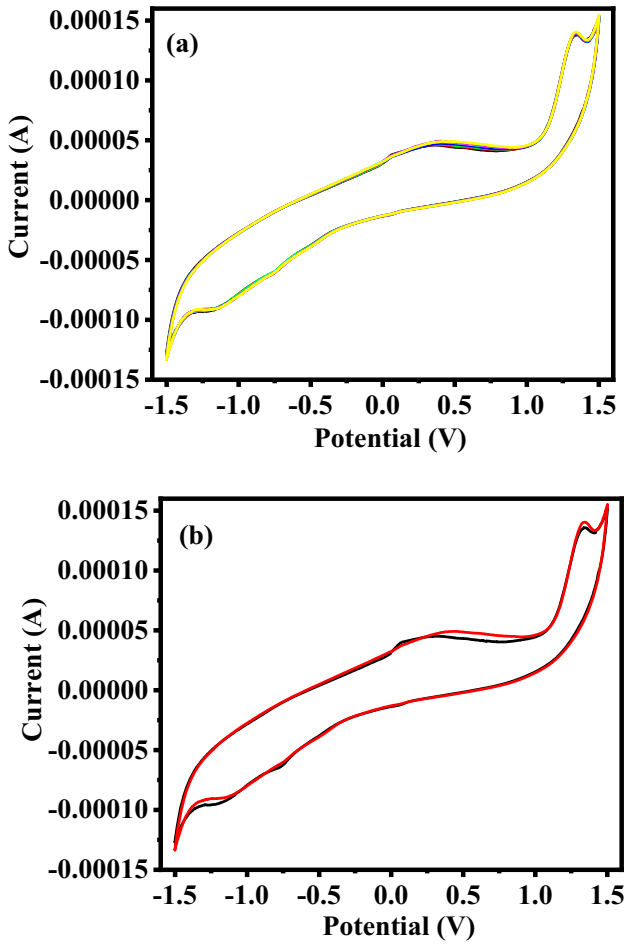

Fig. 8 **a** Seven consecutive cycles of Si-NPs in presence of 62.25 μM (4-NP) in 0.1 M PBS at 100 mV/s, **b** stability test first and after 30 days at the same conditions

when the time span increases with a gradual interval at 200 s, 400 s, 600 s, 800 s, 1000 s, 1200 s and 1400 s current decreases to $-7.32\,10^{-5}$, $-8.68\,10^{-5}$, $-5.39\,10^{-5}$, $-7.07\,10^{-5}$, $-4.46\,10^{-5}$, $4.08\,10^{-5}$ and $-4.46\,10^{-5}$ consequently for Si-NPs/GCE electrode. The current vs time graph of chronoampherometry represent a successive data, reveals that the prepared working electrode for sensing of 4-NP is precise, selective, reproducible, sustainability and reliable for a long time response [48, 49].

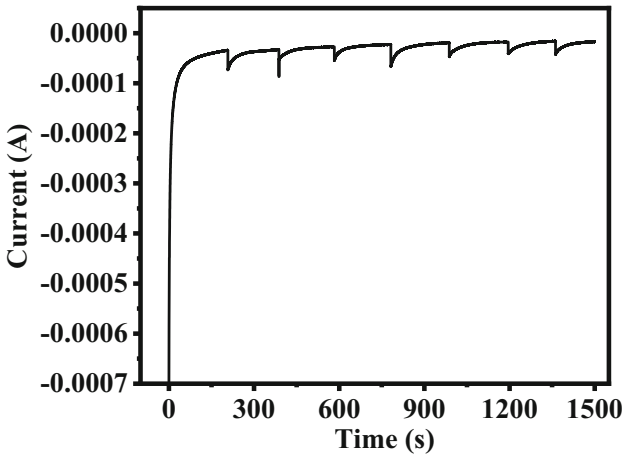

Fig. 9 Amperometric test for the Si-NPs by subsequent additions of in 4-NP in 0.1 M PBS

3.9 Electrochemical impedance spectra (EIS) with Si-NPs/GCE

The Electrochemical impedance spectra (EIS) is a technique to know the working electrode (Si-NPs/GCE) resistance and conductance in presence of a series of different concentrations (7.8, 15.62, 31.25, 62.25, 250, 500 and 1000 μM in 100 mL PBS) of 4-NP with the frequency ranges from 0.01 to 10 kHz (Fig. 10). In the present spectra the X-axis represent

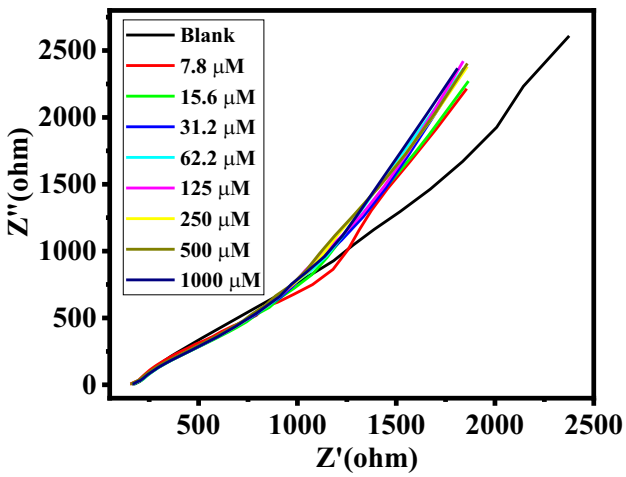

Fig. 10 Electrochemical impedance spectra of Si-NPs modified GCE in 0.1 M PBS at different concentrations of 4-NP (a–h 7.8, 15.62, 31.25, 62.25, 250, 500 and 1000 μM)

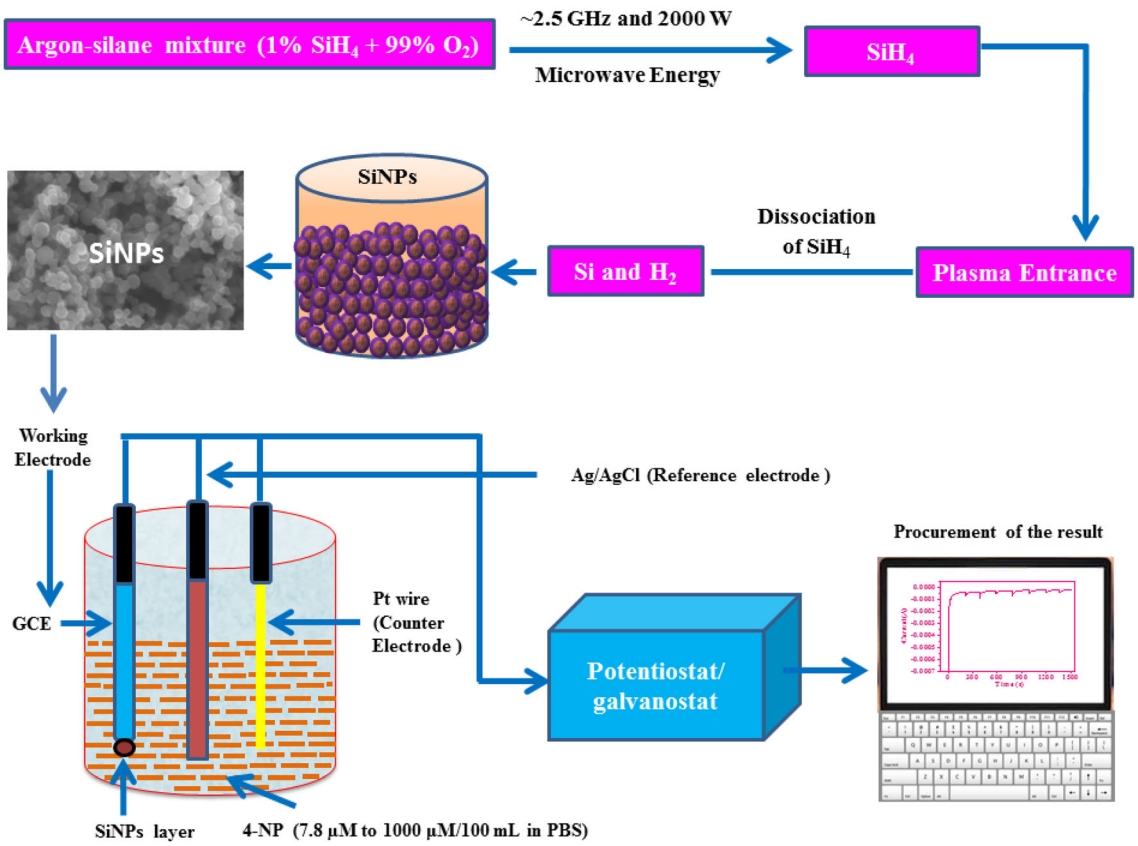

Fig. 11 Schematic flow diagram of experimental setup and sensing and data analysis

the ohmic whereas Y axis shows the capacitive property in the Nyquist plot. It's well documented that the impedance subjected from high to low frequency regions respectively. The result showed that many semicircles like curves of EIS represent that the less charge transfer resistance received from the Si-NPs/GCE electrode. In the present work, the blank sample shows a state line, which describes the less frequency with limited electron-transfer process. When different concentrations of 4-NP were used in the PBS and check the EIS, many wide semicircle are in the high-frequency region was observed and it analogous to electron-transfer at limited process. The semicircles diameter displays the high frequency and resistance charge transfer (Rct), responsible to control the electron transfer rate at electrode interface. It is well-known fact that the larger the semicircle curve illustrates a high interfacial Rct, and resulted a poor electrical conductivity of an active material. The results in the form of curves (Fig. 10) reveals that diameter of semicircle at low nitrophenol concentrations are started and large in size, which is directly associated to the higher concentrations, which may be due to high Rct values in the Si-NPs electrode [50]. The semicircles diameter is increases with increase of concentration of 4-NP, attributes that the Rct value is analogous and directly proportional to the 4-NP concentrations and that's why the Si-NPs exhibit the active high catalytic properties [50].

3.9.1 *Probable mechanism and discussion*

The microwave assisted Si-NPs exhibits very unique characteristic such as high crystallinity, enhanced surface area, good chemical and optical properties [40], which are responsible for the electron transportation and upsurge rate of electrical conductivity [40–42]. The current work displayed the formation of Si-NPs through the utilization of microwave energy. The formed materials crystallinity, structural and functional detail were confirmed via XRD, FESEM, TEM and FTIR spectroscopy respectively as described in the experimental section. The material was successfully applied as a working electrode on GCE as a film form to check their sensing characteristic of 4-NP, which act as an analyte in PBS (as

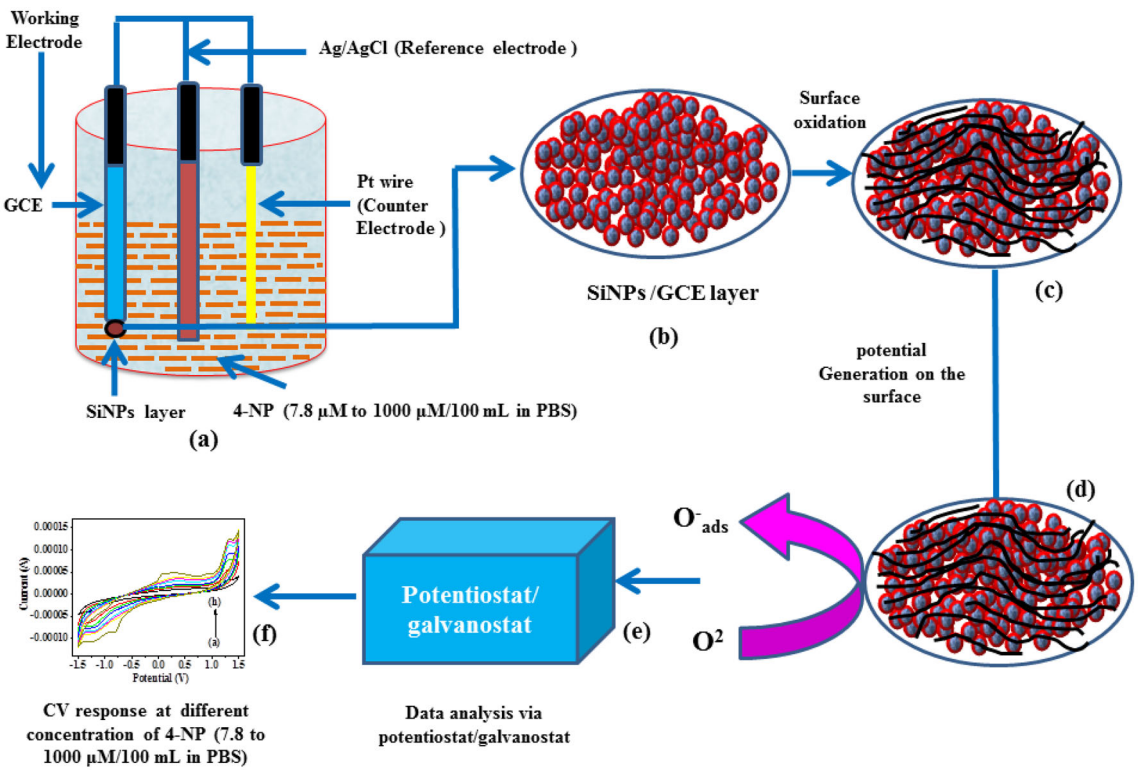

Fig. 12 Schematic sensing mechanism for the Si-NPs with 4NP at different concentration

schematic Fig. 11). It's well documented that the 4-NP is an industrial chemical and have a toxic in nature, therefore, its required and crucial demand to analyze their sensing characteristic via cost effective process [1–4]. For to this a long range of different concentration of 4-NP (7.8, 15.62, 31.25, 62.25, 250, 500 and 1000 µM in 100 mL PBS) was used to check the sensing efficiency and tested in PBS with working electrode (Si-NPs/GCE) through electro chemical detection method. As it's evident, from the cycle test that the processed Si-NPs/GCE exhibit high stability and reproducibility depends upon the performance of formed sensor. Because of the enhanced stability, longer reproducibility, the sensor can be utilized for the environmental and industrial samples to determine the 4-NP easily in a very less time. It's assumed that the developed Si-NPs/GCE electrode is based on the heterogeneous catalyst, where the adsorption and conductance takes place on surface layer of Si-NPs/GCE. Various changes occurred in the spectrum, once the Si-NPs in the form of liquid slurry pasted on GCE and it (Si-NPs/GCE) was immersed in the PBS for to check the current and potential with a varied concentration of analyte (4-NP). The atmospheric oxygen has ability to physio-adsorb on the surface layer of Si-NPs/GCE. It has a probability to interchange the places on surface of Si-NPs/GCE and help to gets ionized (O^-_{ads}) via the elimination of electron from the conduction band and changes into their oxidized (O^- or O^{2-}) form on Si-NPs/GCE surface (as illustrated in Fig. 12). The modified electrode (Si-NPs/GCE) generates a charge layer between the SiNPs and analyte [51, 52]. The Si-NPs/GCE surface adsorbs this oxygen, which exhibit the capability to amplify the potential of Si-NPs/GCE and also to improve the resistance in the formed processed assembly (Fig. 12). Based on the obtained results it leads a reduction in conductance and increase in potential of the formed (Si-NPs/GEC) electrode [51, 52]. In this experiment, once the change in concentration (low to high) of analyte (4-NP) happens, provides higher efficiency. The received sensor data influences on the basis of formed nanostructured geometry, pH, electrolyte, electrode preparation, chemical and physical properties etc. [51, 52]. The Si-NPs exhibit enhanced surface to volume ratio, which increase the band gap, good conductivity, creates a high electron transportation channels and it facilitates higher sensing aptitude [53]. The Si-NPs unveil high affinity and to produce a fruitful environment on their surfaces and

Table 2 4-NPs sensing with different metal, oxide and polymeric materials

S. N	Electrode or catalyst	Nanomaterials	Analyte	Applied Method	Potential or Sensitivity	Detection range or Limit (DL)	Ref
1	Silver Nanowire-PANI/GCE	Silver Nanowire-PANI	4-nitrophenol	CV	−0.77 V	0.6–32 µM	[1]
2	copper-curcumin complex /GCE	CuO and curcumin	4-nitrophenol	CV	1.57 µA/µM/cm	potential range between−0.6 and+ 0.6 V	[2]
3	Mn_2O_3–ZnO nanoparticles/GCE	Mn_2O_3–ZnO nanoparticles	4-nitrophenol	CV	0.1 nM to 50.0 µM	0 to 1.6	[3]
4	Mn-Doped ZnS QDs	Mn-ZnS QDs	4-nitrophenol	CL	–	0.1 to 40 µM	[4]
5	CuO Nano hybrides	CuO	4-nitrophenol	IV	4.50 µA/cm^2/mM	–	[5]
6	Graphene Oxide	GO	4-nitrophenol	CV	–	0.1 to 120 µM	[6]
7	Ce_2O_3 Nano particles Decorated CNT	Ce_2O_3-CNT	2-nitrophenol	CV	1.6×10^{-3}	100 pM ~ 100.0 Mm and	[7]
8	Ag_2O-CNT-NCs/GCE	Ag_2O	p-nitrophenol	CV	103.89 µA/µM/cm^2)	1.0 nM–0.01 mM	[8]
9	Ag_2O–CNT NCs/GCE	Ag_2O-CNT	p-nitrophenol	CV	103.89 µA/µM/cm^2)	1.0 nM–0.01 mM	[8]
10	Ag_2O/GCE	Ag_2O	p-nitrophenol	CV	103.89 µA/µM/cm^2)	1.0 nM–0.01 mM	[8]
11	Ag_2O-CB/GCE	Ag_2O-CB	p-nitrophenol	CV	103.89 µA/µM/cm^2)	1.0 nM–0.01 mM	[8]
12	Ag_2O-GO/GCE	Ag_2O-GO	p-nitrophenol	CV	103.89 µA/µM/cm^2)	1.0 nM–0.01 mM	[8]
13	Ag@Co-Al LDH/PoPD nanohybrids/ GCE	Ag@Co-Al Laye red Double Hydr oxides Rein forc- ed Poly (o-phen ylenediamine)	4-nitrophenol 2,4-DNP UA	DPV DPV DPV	0.82×10^{-9} M–1.74×10^{-6} M 0.1×10^{-6} M–2.5×10^{-6} M 7.55×10^{-7} M 1.23×10^{-5} M	0.82×10^{-9} M–1.74×10^{-6} M 0.1×10^{-6} M–2.5×10^{-6} M 7.55×10^{-7} M–1.23×10^{-5} M	[9]
14	HA-NP/GCE	Hydroxyapatite NP	4-nitrophenol	DPV	1–300 (µM)	0.60 (µM)	[10]
15	Ag-Chitosan/GCE	Ag-Chitosan	4-nitrophenol	SWV	70 nM (DL)	0.07–2.0 (µM)	[11]

Table 2 continued

S. N	Electrode or catalyst	Nanomaterials	Analyte	Applied Method	Potential or Sensitivity	Detection range or Limit (DL)	Ref
16	Nano-Au/GCE	Nano-Au	4-nitrophenol	LSV	10–100 (μM)	8.0 (μM)	[12]
17	Cu_2O-sheets	Cu_2O	4-nitrophenol	DPV	0.006–2.72 (μM)	0.50 (μM)	[13]
18	ZnO-Fe_2O_3 NP/Au/GCE	ZnO-Fe_2O_3 NP/Au	4-nitrophenol	Amperometry	1–10 (μM)	0.83 (μM)	[14]
19	graphitic carbon nitride (O-gC3N4)	Oxidized O-gC_3N_4	4-nitrophenol	DPV	0.0033 to 0.313 μM	0.075 μM (DL)	[15]
20	Porphyrin graphene oxide TiO_2 based Ternary com- posite GO/TiO_2-CuTCPP	GO/TiO_2-CuTCPP	4-nitrophenol	CV	0.0033 to 0.313 μM	0.075 μM (DL)	[16]
21	Boron-doped diamond electrode	Boron	4-nitrophenol	SWV	–	2.8 mg/L (DL)	[17]
22	Cr_2Se_3Hexa gons/modified screen-printed carbon electr- ode (SPCE)	Cr_2Se_3	4-nitrophenol	CV	1.24 μA/μM/cm^2	0.01 μM (DL)	[18]
23	organosilane-functionalized CDs to silica-coated CdSe quantum dots (CdSe@SiO_2) Ratiometric fluorescent sensor	silica-coated CdSe quantum dots (CdSe@SiO_2)	4-nitrophenol	Fluorescence reso nance energy (FRE)	0.051 and 13.7 μg/mL	0.026 μg/mL (DL)	[19]
24	Britton-Robinson buffer (BR)	In Britton-Robinson buffer (BR) of pH 2.0	4-nitrophenol	DPV	2–100 μmol/L	0.17 μmol/L	[20]
25	Acetylene Black Paste with Graphene Hybrid Electrode	Acetylene Black Paste	4-nitrophenol	CV	20 nM to 8.0 μM	8.0 nM (DL)	[21]
26	Ag@Nd_2O_3/Nafion/GCE	Silver doped neodymium oxide	4-nitrophenol	CV	1.0 pM–0.1 mM	0.43 pM (DL)	[22]
27	Biomass-derived activated carbon (AC)	Activated carbon (AC)	4-nitrophenol	CV	5.810 μA/μM/cm^2	0.16 μM	[23]
28	SiNPs/GCE	Silicon NPs (∼4 nm)	4-nitrophenol	CV	7.8–1000 μM	% stability 14.9, % RSD 1.154 0.512 μM (IPc DL) 0.614 μM (IPa DL)	This paper

also allows to access the role of analyte via adsorption process validated the higher rate of electron transportation between the electrode film and analyte (4-NP). The surface of Si-NPs film on GCE activates in the solution of PBS with analyte (4-NP) provides full feasibility. It directly or indirectly affects the reaction/response time reflects in form of their electrical signals/enactment of the produced sensor. The Si-NPs plays a crucial role for to speedy reaction process with initially surface adsorbed oxygen on GCE, also accelerate the conductance and sensing response of 4-NP [51, 52]. A detailed compared table is also presented with different material (metal, oxide and polymeric) sensing with 4-NPs (Table 2), which shows an efficacy of the processed sensor [53–76].

4 Conclusions

The summary of the present work demonstrates that the microwave assisted formed Si-NPs was utilized as a sensing material against industrial compound 4-nitrophenol. The prepared material Si-NPs were well analyzed to access their structural (FESEM and TEM), chemical and electrochemical studies. Initially, the processed nanoparticles (Si-NPs) was characterized via XRD for to access their crystalline, phase and particles diameter of the formed powder, which reveals that the processed material is highly crystalline in nature and have a perfect phases of silicon particle with ~ 4 nm crystallite in size. The morphology of NPs was retrieved through FESEM, which shows that the individual particles size is very small ~ 4 nm with spherical in shape and justifies with size distributation data. The structural detail was further confirmed through TEM and it is well justifies with FESEM observations. The grown powders chemical characteristic in terms of functional detail was also examined via FTIR spectroscopy. The prepared working electrode Si-NPs/GCE was applied to check the sensing detection of 4-NP. The long range of low to high concentration of 4-NP (7.8, 15.62, 31.25, 62.25, 250, 500, 1000 μM in PBS) was opted to check their electrochemical studies, which reveals good feasibility with the Si-NPs/GCE. The effect of different potential was also accessed from 5 to 100 mV with Si-NPs/GCE electrode. The reproducibly and sustainability of formed Si-NPs/GCE were also accessed and found that the formed sensor is in the arrangement of Si-NPs/GCE working electrode exhibit enough stability, reproducible and sustainability for the longer period. The chronoamperometry (0–1500 *s*) and electrochemical impedance spectra (EIS, 7.8 to 1000 μM/100 mL PBS) were also checked, which reveals the performance of formed sensor. Based on the acquired results and their discussions a possible mechanism was also described.

Acknowledgements

The authors are grateful to the Researchers Supporting Project number (RSP-2020/113), King Saud University, Riyadh, Saudi Arabia for the support.

Compliance with ethical standards

Conflict of interest The authors declare that there are no conflicts of interest.

References

1. Q.Q. Li, A. Loganath, Y.S. Chong, J. Tan, J.P. Obbard, Persistent organic pollutants and adverse health effects in humans. J. Toxicol. Environ. Health **69**, 1987–2005 (2006)
2. M. Dunier, A.K. Siwicki, Effects of pesticides and other organic pollutants in the aquatic environment on immunity of fish: a review. Fish Shellfish Immunol. **3**, 423–438 (1993)
3. P. Mulchandani, C.M. Hangarter, Y. Lei, W. Chen, A. Mulchandani, Amperome tric microbial biosensor for p-nitrophenol using *moraxella* sp. modified carbon paste electrode. Biosens. Bioelectron. **21**, 523–527 (2005)
4. M. Castillo, R. Domingues, M.F. Alpendurada, D. Barcelo, Persistence of selected pesticides and their phenolic transformation products in natural waters using offline liquid solid extraction followed by liquid chromatographic techniques. Anal. Chim. Acta **353**, 133–142 (1997)
5. J. Li, D. Kuang, Y. Feng, F. Zhang, Z. Xu, M. Liu, A graphene oxide-based electro chemical sensor for sensitive determination of 4-nitrophenol. J. Hazard Mater. **201**, 250–259 (2012)
6. C.C. Wang, Y.C. Weng, T.C. Chou, Acetone sensor using lead foil as working electrode. Sens. Actuators B **122**, 591–595 (2007)
7. F. Wang, S. Hu, Electrochemical sensors based on metal and semiconductor nanoparticles. Microchim. Acta **165**, 1–22 (2009)
8. U.S. Environmental Protection Agency, *4-nitrophenol, health and environmental effects profile no. 135* (U.S. Environmental Protection Agency, Washington DC, 1980)

9. S. Yi, W.Q. Zhuang, B. Wu, S.T.L. Tay, J.H. Tay, Biodegradation of p-nitrophenol by aerobic granules in a sequencing batch reactor. Environ. Sci. Technol. **40**, 2396 (2006)
10. J.A. Herrera-Melian, J.M. Dona-Rodriguez, E.T. Rendon, A. S. Vila, M.B. Quetglas, A.A. Azcarate, L.P. Pariente, Solar photocatalytic destruction of p-nitrophenol: a pedagogical use of lab wastes. J. Chem. Educ. **78**, 775 (2001)
11. L. Bo, X. Quan, S. Chen, H. Zhao, Y. Zhao, Degradation of p-nitrophenol in aqueous solution by microwave assisted oxidation process through a granular activated carbon fixed bed. Water Res. **40**, 3061–3068 (2006)
12. M.A. Quiroz, S. Reyna, C.A. Martiinez-Huitle, S. Ferro, A.D. Battisti, Electro catalytic oxidation of p-nitrophenol from aqueous solutions at Pb/PbO_2 anodes. Appl. Catal. B **59**, 259–266 (2005)
13. X. Wang, H. Zhao, X. Quan, Y. Zhao, S. Chen, Visible light photoelectro catalysis with salicylic acid-modified TiO_2 nanotube array electrode for p-nitrophenol degradation. J. Hazard Mater. **166**, 547–552 (2009)
14. M.A. Oturan, J. Peiroten, P. Chartrin, A.J. Acher, Complete destruction of p-nitrophenol in aqueous medium by electro-fenton method. Environ. Sci. Technol. **34**, 3474–3479 (2000)
15. F.C. Moraes, S.T. Tanimoto, G.R. Salazar-Band, S.A.S. Machado, L.H. Mascaro, A new indirect electroanalytical method to monitor the contamination of natural waters with 4-nitrophenol using multiwall carbon nanotubes. Electroanalysis **21**, 1091–1098 (2009)
16. Z. Liu, J. Du, C. Qiu, L. Huang, H. Ma, D. Shen, Y. Ding, Electrochemical sensor for detection of p-nitrophenol based on nanoporous gold. Electrochem. Commun. **11**, 1365–1368 (2009)
17. G. Liu, Y. Lin, Electrochemical sensor for organophosphate pesticides and nerve agents using zirconia nanoparticles as selective sorbents. Anal. Chem. **77**, 5894–5901 (2005)
18. K. Esumi, R. Nakamura, A. Suzuki, K. Torigoe, Preparation of platinum nanoparticles in ethyl acetate in the presence of poly (amidoamine) dendrimers with a methyl ester terminal group. Langmuir **16**, 7842–7846 (2010)
19. S. Wunder, F. Polzer, Y. Lu, Y. Mei, M. Ballauff, Kinetic analysis of catalytic reduction of 4-nitrophenol by metallic nanoparticles immobilized in spherical polyelectrolyte brushes. J. Phys. Chem. C **114**, 8814–8820 (2010)
20. S. Wunder, Y. Lu, M. Albrecht, M. Ballauff, Catalytic activity of faceted gold nanoparticles studied by a model reaction: evidence for substrate-induced surface restructuring. ACS Catal. **1**, 908–916 (2011)
21. J. Kaiser, L. Leppert, H. Welz, F. Polzer, S. Wunder, N. Wanderka, M. Albrecht, T. Lunkenbein, J. Breu, S. Kummel, Y. Lu, M. Ballauff, Catalytic activity of nanoalloys from gold and palladium. Phys. Chem. Chem. Phys. **14**, 6487–6495 (2012)
22. N.C. Antonels, R. Meijboom, Preparation of well-defined dendrimer encap- sulated ruthenium nanoparticles and their evaluation in the reduction of 4-nitrophenol according to the langmuir-hinshelwood approach. Langmuir **29**, 13433–13442 (2013)
23. P. Ncube, N. Bingwa, H. Baloyi, R. Meijboom, Catalytic activity of palladium and gold dendrimer-encapsulated nanoparticles for methylene blue reduction: a kinetic analysis. Appl. Catal. A **495**, 63–71 (2015)
24. N. Bingwa, R. Meijboom, Kinetic evaluation of dendrimer-encapsulated pall adium nanoparticles in the 4-nitrophenol reduction reaction. J. Phys. Chem. C **118**, 19849–19858 (2014)
25. A. Niazi, A. Yazdanipour, Spectrophotometric simultaneous determination of nitrophenol isomers by orthogonal signal correction and partial least squares. J. Hazardous Mater. **146** (1–2), 421–427 (2007)
26. M.J. Thompson, L.N. Ballinger, S.E. Cross, M.S. Roberts, High-performance liquid chromatographic determination of phenol, 4-nitrophenol, β-naphthol and a number of their glucuronide and sulphate conjugates in organ perfusate. J. Chromatogr. B **677**(1), 117–122 (1996)
27. W. Zhang, C.R. Wilson, N.D. Danielson, Indirect fluorescent determination of selected nitro-aromatic and pharmaceutical compounds via UV-photolysis of 2 phenylbenzimidazole-5-sulfonate. Talanta **74**(5), 1400–1407 (2008)
28. J.A.P. Sánchez, P.P. Bolaños, R.R. González, A.G. Frenich, J. L.M. Vidal, Application of a quick, easy, cheap, effective, rugged and safe based method for the simultaneous extraction of chlorophenols, alkylphenols, nitrophenols and cresols in agricultural soils, analyzed by using gas chromatography–triple quadrupole mass spectrometry/mass spectrometry. J. Chromatogr. A **1217**(36), 5724–5731 (2010)
29. X. Guo, Z. Wang, S. Zhou, The separation and determination of nitrophenol isomers by high-performance capillary zone electrophoresis. Talanta **64**(1), 135–139 (2004)
30. S. Singh, N. Kumar, V.K. Meena, C. Kranz, S. Mishra, Impedometric phenol sensing using graphenated electrochip. Sens. Actuators B **237**, 318–328 (2016)
31. P.G. Jeelani, P. Mulay, R. Venkat, C. Ramalingam, (2019) Multifaceted application of silica nanoparticles. A review. Silicon (2019). https://doi.org/10.1007/s12633-019-00229-y
32. M.H. Nayfeh, L. Mitas, Silicon nanoparticles: new photonic and electronic material at the Transition between solid and molecule, *Nanosilicon* (Elsevier, Amsterdam, 2008), pp. 1–78

33. C. Huan, S.S. Qing, (2014) Silicon nanoparticles: preparation, properties, and applications. Chin. Phys. B **23**(8), 088102 (2014)
34. J. Knipping, H. Wiggers, B. Rellinghaus, P. Roth, D. Konjhodzic, C. Meier, Synthesis of high purity silicon nanoparticles in a low pressure microwave reactor. J. Nanosci. Nanotechnol. **4**(4), 1039–1044 (2004)
35. D.D. Lovingood, J.R. Owens, M. Seeber, K.G. Kornev, I. Luzinov, Preparation of silica nanoparticles through microwave-assisted acid-catalysis. J. Vis. Exp. **82**, 51022 (2013)
36. D.D. Lovingood, J.R. Owens, M. Seeber, K.G. Kornev, I. Luzinov, Controlled micro-wave-assisted growth of silica nanoparticles under acid catalysis. ACS Appl. Mater. Interfaces **4**(12), 6875–6883 (2012)
37. Y.J. Zhu, F. Chen, Microwave-assisted preparation of inorganic nanostructures in liquid phase. Chem. Rev. **114**(12), 6462–6555 (2014)
38. R. Wahab, N. Ahmad, M. Alam, A.A. Ansari, Nanocubic magnesium oxide: towards hydrazine sensing. Vacuum **155**, 682–688 (2018)
39. A. Gupta, H. Wiggers, Freestanding silicon quantum dots: origin of red and blue luminescence. Nanotechnology **22**(5), 055707 (2010)
40. S. Hartner, A. Gupta, H. Wiggers, *Electrical Properties of Functionalized Silicon Nanoparticles*, vol. 1 (NSTI-Nanotech, 2010). www.nsti.org
41. B. Giesen, H. Wiggers, A. Kowalik, P. Roth, Formation of Si-nanoparticles in a microwave reactor: comparison between experiments and modelling. J. Nanoparticle Res. **7**, 29–41 (2005)
42. A. Münzer, J. Sellmann, P. Fortugno, A. Kempf, C. Schulz, H. Wiggers, Inline coating of silicon nanoparticles in a plasma reactor: reactor design, simulation and experiment. Mater. Today Proc. **4**, S118–S127 (2017)
43. A.J. Ghazizadeh, A. Afkhami, H. Bagheri, Voltammetric determination of 4-nitrophenol using a glassy carbon electrode modified with a gold-ZnO–SiO_2 nanostructure. Mikrochim. Acta **185**(6), 296 (2018). https://doi.org/10.1007/s00604-018-2840-4
44. Y. Hana, Y. Chen, J. Feng, M. Na, J. Liu, Y. Ma, S. Ma, X. Chen, Investigation of nitrogen content effect in reducing agent to prepare wavelength controllable fluorescent silicon nanoparticles and its application in detection of 2-nitrophenol. Talanta **194**, 822–829 (2019)
45. A.J. Ghazizadeh, A. Afkhami, H. Bagheri, Voltammetric determination of 4-nitrophenol using a glassy carbon electrode modified with a gold-ZnO–SiO_2 nanostructure. Microchim. Acta **185**, 296 (2018)
46. N.I. Ikhsan, P.R. Kumar, N.M. Huang, Controlled synthesis of reduced graphene oxide supported silver nanoparticles for selective and sensitive electrochemical detection of 4-nitrophenol. Electrochim. Acta **192**, 392–399 (2016)
47. D. Saikia, Y.Y. Huang, C.E. Wua, H.M. Kao, Size dependence of silver nanoparticles in carboxylic acid functionalized mesoporous silica SBA-15 for catalytic reduction of 4-nitrophenol. RSC Adv. **6**, 35167–35176 (2016)
48. A. Mejri, A. Mars, H. Elfil, A.H. Hamzaoui, Voltammetric simultaneous quantification of p-nitrophenol and hydrazine by using magnetic spinel $FeCo_2O_4$ nanosheets on reduced graphene oxide layers modified with curcumin-stabilized silver nanoparticles. Microchim. Acta **186**, 561 (2019)
49. M. Pabbi, S.K. Mittal, An electrochemical algal biosensor based on silica coated ZnO quantum dots for selective determination of acephate. Anal Methods **9**, 1672–1680 (2017)
50. T. Muthukumar, M. Shenbagapushpam, S.B. Madasamy, M. M. Paulpandian, S. Kodirajan, Fabrication of hard bound mesoporous silica stabilized Cu(I) electrocatalyst for 4-nitrophenol sensor via alcothermal strategy, Fabrication of hard bound meso porous silica stabilized Cu(I) electrocatalyst for 4-nitrophenol sensor via alcothermal strategy. J. Electroanal. Chem. **859**, 113792 (2020)
51. S.G. Ansari, R. Wahab, Z.A. Ansari, Y.S. Kim, G. Khang, A. Al-Hajry, H.S. Shin, Effect of nanostructure on the urea sensing properties of sol–gel synthesized ZnO. Sens. Actuators B **137**, 566–573 (2009)
52. S. Chaudhary, A. Umar, K.K. Bhasin, S. Baskoutas, Chemical sensing applications of ZnO nanomaterials. Materials **11**, 287 (2018). https://doi.org/10.3390/ma11020287
53. A. Umar, F.A. Harraz, A.A. Ibrahim, T. Almas, R. Kumar, M. S. Al-Assiri, S. Baskoutas, Iron-doped titanium dioxide nanoparticles as potential scaffold for hydrazine chemical sensor applications. Coatings **10**, 182 (2020). https://doi.org/10.3390/coatings10020182
54. C. Zhang, S. Govindaraju, K. Giribabu, Y.S. Huh, K. Yun, AgNWs-PANI nanocomposite based electrochemical sensor for detection of 4-nitrophenol. Sens. Actuators B **252**, 616–623 (2017)
55. B. Dinesh, R. Saraswathi, Electrochemical synthesis of nanostructured copper–curcumin complex and its electrocatalytic application towards reduction of 4-nitrophenol. Sens. Actuators B **253**, 502–512 (2017)
56. M.M. Rahman, G. Gruner, M.S. Al-Ghamdi, M.A. Daous, S. B. Khan, A.M. Asiri, Chemo-sensors development based on low-dimensional codoped Mn_2O_3–ZnO nanoparticles using flat-silver electrodes. Chem. Central J. **7**, 1–12 (2013)
57. J. Liu, H. Chen, Z. Lin, J.M. Lin, Preparation of surface imprinting capped Mn-doped ZnS quantum dots and their application for chemiluminescence detection of 4-nitrophenol in tap water. Anal. Chem. **82**(17), 7380–7386 (2010)

58. S.B. Khan, M.M. Rahman, K. Akhtar, A.M. Asiri, K.A. Alamry, J. Seo, H. Han, Copper oxide basedpolymer nanohybridfor chemical sensor applications. Int. J. Electrochem. Sci. **7**, 10965–10975 (2012)
59. J. Li, D. Kuang, Y. Feng, F. Zhang, Z. Xu, M. Liu, A graphene oxide-based electrochemical sensor for sensitive determination of 4-nitrophenol. J. Hazard Mater. **201–202**, 250–259 (2012)
60. M.M. Hussain, M.M. Rahman, A.M. Asiri, Efficient 2-nitrophenol chemical sensor development based on Ce_2O_3 nanoparticles decorated CNT nano composites for environmental safety. PLoS ONE **11**(12), e0166265 (2016). https://doi.org/10.1371/journal.pone.0166265
61. M.M. Rahman, H.M. Marwani, F.K. Algethami, A.M. Asiri, S.A. Hameed, B. Alhogbi, Ultra-sensitive p-nitrophenol sensing performances based on various Ag_2O conjugated carbon material composites. Environ. Nanotechnol. Monit. Manage. **8**, 73–82 (2017)
62. T. Dhanasekaran, R. Manigandan, A. Padmanaban, R. Suresh, K. Giribabu, V. Narayanan, Fabrication of Ag@Co-Al layered double hydroxides reinforced poly (o-phenylene di amine) nanohybrid for efficient electrochemical detection of 4-nitrophenol, 2,4-dinitrophenol and uric acid at nano molar level. Sci. Rep. **9**, 13250 (2019)
63. H. Yin, Y. Zhou, S. Ai, X. Liu, L. Zhu, L. Lu, Electrochemical oxidative determination of 4-nitrophenol based on a glassy carbon electrode modified with a hydroxyapatite nanopowder. Microchim. Acta **169**, 87–92 (2010)
64. C.A. De Lima, P.S. da Silva, A. Spinelli, Chitosan-stabilized silver nanoparticles for voltammetric detection of nitrocompounds. Sens. Actuators B **196**, 39 (2014)
65. L. Chu, L. Han, X. Zhang, Electrochemical simultaneous determination of nitro phenol isomers at nano-gold modified glassy carbon electrode. J. Appl. Electron. Chem. **41**, 687 (2011)
66. V. Veeramani, M. Sivakumar, S.M. Chen, R. Madhu, Z.C. Dai, N. Miyamoto, A facile electrochemical synthesis strategy for Cu_2O (cubes, sheets and flowers) microstructured materials for sensitive detection of 4-nitrophenol. Anal. Methods **8**, 5906–5910 (2016)
67. K. Singh, A. Kaur, A. Umar, G.R. Chaudhary, S. Singh, S.K. Mehta, A comparison on the performance of zinc oxide and hematite nanoparticles for highly selective and sensitive detection of para-nitrophenol. J. Appl. Electrochem. **45**, 253–261 (2015)
68. M. Ramalingam, V.K. Ponnusamy, S.N. Sangilimuthu, Electrochemical determination of 4-nitrophenol in environmental water samples using porous graphitic carbon nitride-coated screen-printed electrode. Environ. Sci. Pollut. Res. **27**, 17481–17491 (2020)
69. J. Chen, Y. Lu, L. Huang, Z. Shi, Y. Zheng, X. Song, C. Wu, Z. Wu, Photo catalytic self-cleaning electrochemical sensor for 4-nitrophenol detection. Int. J. Electrochem. Sci. **15**, 5179–5192 (2020)
70. V.D. Pedrosa, L. Codognoto, L.A. Avaca, Electroanalytical determination of 4-nitrophenol by square wave voltammetry on diamond electrodes. J. Braz. Chem. Soc. **14**(4), 530–535 (2003)
71. S. Ramaraj, S. Mani, S.M. Chen, S. Palanisamy, V. Velusamy, J.M. Hall, T.W. Chen, T.W. Tseng, Hydrothermal synthesis of Cr_2Se_3 hexagons for sensitive and low level detection of 4-nitrophenol in water. Sci. Rep. **8**, 4839 (2018)
72. M. Liu, Z. Gao, Y. Yu, R. Su, R. Huang, W. Qi, Z. He, Molecularly imprinted core-shell CdSe@SiO_2/CDs as a ratiometric fluorescent probe for 4-nitro phenol sensing. Nanoscale Res. Lett. **13**, 27 (2018)
73. R. Pfeifer, P.T. Martinhon, C. Sousa, J.C. Moreira, M.A.C.D. Nascimento, J. Barek, Differential pulse voltammetric determination of 4-nitrophenol using a glassy carbon electrode: comparative study between cathodic and anodic quantification. Int. J. Electrochem. Sci **10**, 7261–7274 (2015)
74. Q. He, Y. Tian, Y. Wu, J. Liu, G. Li, P. Deng, D. Chen, Facile and ultra sensitive determination of 4-nitrophenol based on acetylene black paste and graphene hybrid electrode. Nanomaterials **9**, 429 (2019)
75. M.M. Rahman, A. Wahid, M.M. Alam, A.M. Asiri, Efficient 4-Nitrophenol sensor development based on facile Ag@Nd2O3 nanoparticles. Mater. Today Commun. **16**, 307–313 (2018)
76. R. Madhu, C. Karuppiah, S.M. Chen, P. Veerakumar, S.B. Liu, Electrochemical detection of 4-nitrophenol based on biomass derived activated carbons. Anal. Methods **6**, 5274–5280 (2014)